Precise Calculations of the Existence of Multiple AMOC Equilibria in Coupled Climate Models. Part II: Transient Behavior

WILLEM P. SIJP AND MATTHEW H. ENGLAND

Climate Change Research Centre, University of New South Wales, Sydney, New South Wales, Australia

(Manuscript received 29 December 2010, in final form 18 April 2011)

ABSTRACT

In Part I of this paper an evolution equation for the Atlantic salinity and the reverse cell strength in the North Atlantic Deep Water (NADW) OFF state was formulated. Here, an analytical solution to this equation is used to test its validity in the context of transient solutions. In this study several transient scenarios in the general circulation model are examined to determine the accuracy of the predictions made with the material in Part I. The authors also determine how well the basic premises of Part I hold throughout these transient behaviors. The unstable equilibria $\overline{S}_{\text{unst}}$ that mark the upper boundary of the OFF state attraction basin are elucidated by the time-dependent behavior shown here. Transient equilibration from one stable NADW OFF state to another in response to changes in the anomalous salt flux H is accurately described by the evolution equation. The theory also explains the distribution of decay times for the NADW OFF state around the maximum critical Atlantic surface flux. Exceedingly long collapse times in excess of 50 000 years are found for surface flux values slightly in excess of the critical value.

1. Introduction

In Sijp et al. (2012; hereafter, Part I) the hysteresis of a climate model of intermediate complexity was examined by equilibration under a fixed anomalous salt flux H applied to the North Atlantic for a range of values. This elucidated the domain of existence of the North Atlantic Deep Water (NADW) ON and OFF state. The total salt exchange between the Atlantic and the Southern Ocean F_{circ} counters changes in the net Atlantic surface flux F_s and depends on the volume-averaged upper-ocean Atlantic salinity $\overline{S}$ (see Table 1 for an explanation of the terms). The highest value H^* where the OFF state exists was calculated from $\partial F_{\text{circ}}/\partial S = 0$. The closed Atlantic salt budget allowed the formulation of a simple evolution equation for $\overline{S}_t$, the average upper Atlantic salinity as a function of time t. This equation also describes the evolution of the Antarctic Intermediate Water (AAIW) reverse cell strength M via Eq. (2) of Part I (see also Table 2). The simplicity of this approach allows an analytical solution to the evolution equation to be found. We will compare analytical solutions of the evolution equation to equivalent time-dependent numerical model behavior. Analytical solutions fall into two categories: one that provides stable (that is nonsingular) solutions for certain initial conditions of $\overline{S}$, and another where all initial conditions eventually evolve toward a singularity. We will examine both categories. We find that the evolution equation describes transitions between stable OFF states, and that the time before the OFF state collapses becomes exceedingly large for net Atlantic surface flux values F_s close to the critical Atlantic surface flux F_s^* (see Table 1).

Four basic premises allowed us to formulate a simple evolution equation for Atlantic salinity $\overline{S}$ in Part I. For convenience, they are stated here:

1) the salinities of the NADW formation region and the South Atlantic (between 30°S and the equator) remain linearly related to $\overline{S}$ under changes in H;
2) the properties of cool fresh AAIW constituting the lower branch of the reverse cell remains relatively unchanged compared to Atlantic surface salinity under changes in H;
3) the strength of the reverse cell M depends linearly on the density difference $\Delta\rho_{\text{NADW}-\text{AAIW}}$ between the NADW and the AAIW formation region;
4) the term F_r acts linearly to reduce the salinity difference between the South Atlantic and the Southern

Corresponding author address: Willem P. Sijp, Climate Change Research Centre (CCRC), University of New South Wales, Sydney, NSW 2052, Australia.
E-mail: w.sijp@unsw.edu.au

DOI: 10.1175/2011JCLI4246.1

© 2012 American Meteorological Society

Unauthenticated | Downloaded 04/20/21 11:40 AM UTC

TABLE 1. The main terms from Part I. Positive sign of flux terms indicate salt added to ocean.

Term	Explanation
$\overline{S}$	Basinwide volume-average upper Atlantic salinity.
M	AAIW reverse cell strength (OFF state only).
M_0	Small M where F_m becomes 0 [Eq. (1)].
H	Added salt flux to NADW region.
H^*	Maximal H where stable OFF state occurs. Similar for F_s^*.
$\overline{S}^*$	$\overline{S}^* = -(b/2a)$. Maximal salinity where stable OFF state occurs; 34.63 kg m^{-3} here.
β	Climate amplification of H such that $\Delta F_s = (1 + \beta)H$.
$\overline{S}_{\text{unst}}$	$\overline{S}_{\text{unst}} = [-b + \sqrt{b^2 - 4a(c + F_s)}]/2a$; salinity at unstable flux equilibrium.
F_s	Total net Atlantic surface salt flux.
F_m	AMOC-related salt flux (ON and OFF) $\int V\langle S\rangle_x \, dz$ at 30°S.
F_r	Residual term $-F_s - F_m$ composed largely of Atlantic gyre salt transport across 30°S.
F_{circ}	Total Atlantic oceanic salt exchange $F_r + F_m$. Balances as $F_{\text{circ}} + F_s = 0$.

Ocean to zero and so causes $\overline{S}$ to tend toward a certain $\overline{S}_r$;

5) North Atlantic density changes are dominated by salinity.

These assumptions led us to three basic linear equations and an evolution equation. For convenience, the main mathematical terms in Table 1 and the key equations in Table 2 are listed.

We will examine transient behavior arising from our evolution equation. Transient behavior predicted by simplified sets of equations has been studied for instance in box models by Lucarini and Stone (2005a,b), Zickfeld et al. (2004), and Colin de Verdière (2010). Lucarini and Stone (2005a) use the box model of Rooth (1982) for a qualitative study of time-dependent Atlantic Meridional Overturning Circulation (AMOC) behavior in the NADW ON state. In qualitative agreement with general circulation model results (Stocker and Schmittner 1997), they find that fast increases in moisture fluxes to the North Atlantic are more effective in shutting down NADW than slow increases, as with high rates of heat flux increases. Zickfeld et al. (2004) take the box model of Rahmstorf (1996), specify the volumes of the boxes, and determine the remaining parameters by a least squares fit of the hysteresis curve to the output of a coupled climate model of intermediate complexity [Climate and Biosphere Model 2 (CLIMBER-2)]. Weights are used to enforce a closer fit near certain regions of the hysteresis curve, for instance near the bifurcation point. Their approach allows a high number of sensitivity tests, for instance relating to the AMOC sensitivity to modified regional patterns of warming, initial conditions, and the rate of climate change. Their box model qualitatively reproduces the result of Stocker and Schmittner (1997), who demonstrated that the stability of the AMOC is dependent upon the rate of climate change.

TABLE 2. The main equations from Part I.

Eq. No.	Equation
1	$F_m = (v_1\overline{S} + v_2)(M - M_0)$
2	$M = d_1\overline{S} + d_2$
3	$F_r = r_1(\overline{S} - \overline{S}_r) = r_1\overline{S} + r_2$
4	$V_{\text{Atl}}(\partial\overline{S}/\partial t) = F_m + F_r + F_s = a\overline{S}^2 + b\overline{S} + (c + F_s)$

The studies of transient behavior by Zickfeld et al. (2004) and Lucarini and Stone (2005a,b) examine transient behavior of the NADW ON state such as collapse and recovery under climate change. In the present study, transient model behavior in the OFF state is examined to validate our equation of motion [Eq. (4) in Part I]. We seek quantitative agreement between certain time-dependent behaviors following from our equation of motion [Eq. (4) in Part I and Table 2] and those exhibited by the three-dimensional coupled numerical model used. Where possible, attempts are made to explain any discrepancies in terms of violations of our basic premises 1–4 (Part I). These tests are intended to further validate the approach described in Part I. Once validated, our framework can be used and expanded in future studies for parameter sensitivity studies to examine the existence of the OFF state under different scenarios.

2. The model and experimental design

We use the intermediate complexity coupled model described in detail in Weaver et al. (2001). This consists of an ocean general circulation model [Geophysical Fluid Dynamics Laboratory Modular Ocean Model (GFDL MOM) Version 2.2; Pacanowski 1995] coupled to a simplified one-layer energy–moisture balance model for the atmosphere and a dynamic–thermodynamic sea ice model of global domain and horizontal resolution 3.6° longitude by 1.8° latitude. Heat and moisture advection takes place via advection and Fickian diffusion. Air–sea heat and freshwater fluxes evolve freely in the model, yet a noninteractive wind field is employed. The wind forcing is taken from the National Centers for Environmental Prediction–National Center for Atmospheric Research (NCEP–NCAR) reanalysis fields (Kalnay et al. 1996), averaged over the period 1958–97 to form a seasonal cycle from the monthly fields. Vertical mixing in the control case is represented using a diffusivity that increases with depth, taking a value of 0.3 cm^2 s^{-1} at the surface and increasing to 1.3 cm^2 s^{-1} at the bottom. We use version 2.8 of the University of Victoria (UVic) model. The effect of subgrid-scale eddies on tracer transport is modeled by the parameterizations of Gent

Unauthenticated | Downloaded 04/20/21 11:40 AM UTC

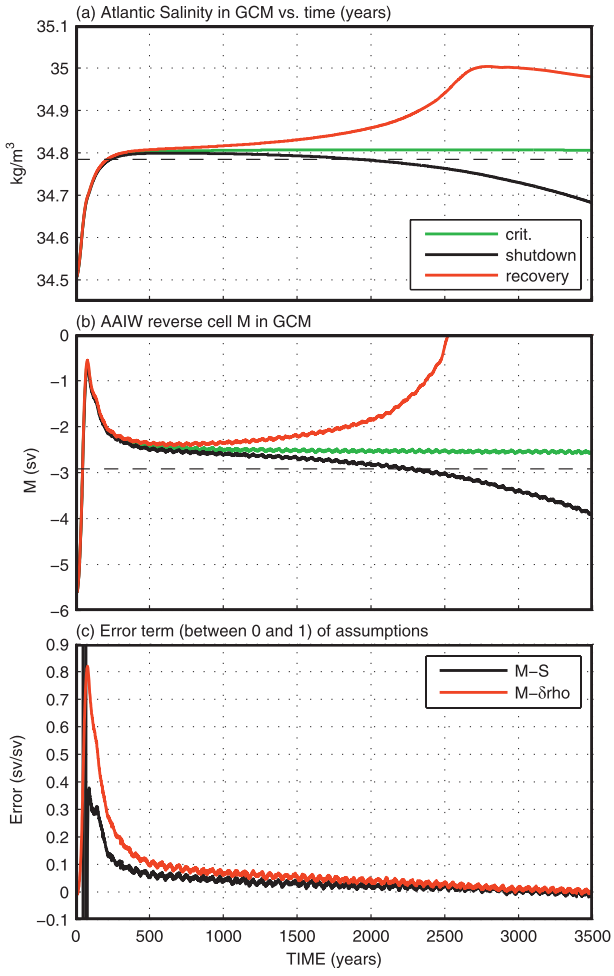

FIG. 1. Results of North Atlantic salt pulse experiments to find the unstable equilibrium S_{unst} on the unstable OFF state branch in the numerical model under fixed anomalous flux $H = 0.0312$ Sv. (a) Atlantic salinity $\overline{S}$ as a function of time t for three 80-yr pulses of similar values leading to a salinity $\overline{S}$ around 34.8 kg m^{-3}. (b) The AAIW reverse cell strength M as a function of time t. (c) The error indicator $[M(\overline{S}) - M_{\text{gcm}}]/M_{\text{gcm}}$, where $M(\overline{S})$ is M calculated from $\overline{S}$ via Eq. (2) (Part I), and M_{gcm} is the AAIW reverse cell strength diagnosed from the numerical model.

and McWilliams (1990). We will refer to this model as ''the numerical model'' to distinguish it from our conceptual model. A detailed outline of the experimental procedure used here is contained in Part I of this paper.

3. A test for the existence of the attraction basin

In Part I two equilibrium solutions $\overline{S}$ and $\overline{S}_{\text{unst}}$ to the evolution Eq. (4) (of Part I, see also Table 2) were found, where initial conditions $\overline{S}_{t=0} < \overline{S}_{\text{unst}}$ are expected to evolve toward $\overline{S}$, while $\overline{S}_t$ encounters a singularity and so evolves to the ON state for $\overline{S}_{t=0} < \overline{S}_{\text{unst}}$. It is impossible to arrive at the unstable equilibria S_{unst} directly in the numerical model. However, their values may be found via transient numerical experiments. The model should spend a particularly long time near this unstable flux-equilibrium state after an excitation by a salt pulse of the right magnitude. This is because small salinity perturbations grow or decay approximately exponentially around any average Atlantic salinity where the salt fluxes are balanced (see Part I and below). This growth is initially small for values very close to a particular salinity where salt fluxes are balanced, as in S_{unst} studied here.

To examine the role of the unstable OFF branch, we conduct experiments where an 80-year-long anomalous salt flux to the North Atlantic is applied for a certain F_s to obtain an initial condition close to that of the unstable OFF branch salinity at the chosen F_s. The pulse consists of a simple triangular profile as described in Sijp and England (2006, 2008), peaking at year 40. It is not a priori clear that this approach is valid, as the salt pulse will likely cause a violation of Eqs. (1)–(3) in Part I. Therefore, to track how well some of our premises are satisfied at each time during transient behavior, an error indicator $[M(\overline{S}) - M_{\text{GCM}}]/M_{\text{GCM}}$ is computed, where $M(\overline{S})$ is the M computed from $\overline{S}$ via Eq. (2) in Part I and M_{GCM} is the AAIW reverse cell strength in the model. We refer to this as the M-S error indicator and take it as a measure of the validity of our basic Eq. (2) (Part I), which encapsulates a linear dependence of M on $\rho_{\text{NADW}} - \rho_{\text{AAIW}}$ and our assumption about a linear relationship between the average Atlantic salinity and the average salinity at the NADW formation sites. Note that the connection between the average Atlantic salinity and the gyre salt flux F_r [Eq. (3)] is not incorporated in this error indicator. Additional errors here may arise from the time it takes for a salinity anomaly in the North Atlantic to travel to the South Atlantic.

To isolate the component of the M-S error indicator arising from a violation of the linear relationship between M and $\rho_{\text{NADW}} - \rho_{\text{AAIW}}$ on our error indicator, an ''M-rho'' error indicator $(M(\Delta\rho) - M_{\text{GCM}})/M_{\text{GCM}}$ is also computed, where $M(\Delta\rho)$ is the reverse cell strength M computed from $\Delta\rho = \rho_{\text{NADW}} - \rho_{\text{AAIW}}$ as shown in Fig. 6 of Part I. When conducting our pulse experiments, the error indicators are tracked to see how well our OFF state premises hold, and so judge whether conclusions can be drawn from our transient experiments.

Figure 1 shows the evolution in response to the short salt pulse of the Atlantic salinity and the AAIW reverse cell strength M in the model as a function of time, along with the two error indicators. We use the anomalous salt flux $H = 0.0312$ Sv (1 Sv $\equiv 10^6$ m^3 s^{-1}) salt equivalent, a value between $H = 0$ and the critical H^* (see Fig. 12 of Part I) where $\overline{S}_{\text{unst}}$ is reasonably close to $\overline{S}$ and should be easily accessible. The short salt pulses are superimposed

Unauthenticated | Downloaded 04/20/21 11:40 AM UTC

on this. We have chosen a small range of salt pulses where the larger pulse led to a transition to the ON state (red), and a smaller pulse led to a collapse back onto the OFF state (black). There is an intermediate pulse (green) leading to an evolution that lingers around a salinity of 34.8 kg m^{-3} (Fig. 5a in Part I) for about 8000 years (not visible because of figure scale), before eventually collapsing back to the OFF state. As expected, the error indicators (Fig. 1c) are large during the initial perturbation, but settle down below 0.1 by year 500. The initial *M*-rho error is significantly lower than the *M-S* error, and close scrutiny reveals that the initial *M*-rho error appears to incorporate a time lag of M behind $\Delta\rho$ of around 30 years. The strong responsiveness of the AAIW reverse cell strength to NADW formation region density is remarkable.

The average Atlantic salinity $\overline{S}$ reaches a plateau around year 500, where the M-S error indicator has becomes small. This suggests that $\overline{S}_{t=500\text{yr}}$ can be taken around this year as an initial condition for the model's subsequent behavior where our basic premises about the OFF state hold (allowing us to apply the unstable OFF branch salinity $\overline{S}_{\text{unst}}$ as an explanation for the bifurcation behavior). The spread in values of the initial condition $\overline{S}_{t=500\text{yr}}$ allows us to examine different behaviors where the system makes a transition to the ON state (red), or collapses back onto the OFF state (black). The bifurcation between these two behaviors occurs around a salinity of 34.8 kg m^{-3} (Fig. 1a) The dashed line in Fig. 1a indicates the unstable equilibrium OFF branch salinity predicted by Eq. (5) (Part I), and is in very good agreement with the model behavior. The associated behavior of the AAIW reverse cell strength *M* (Fig. 1b) exhibits a similarly good agreement, with a slight offset from the calculated unstable branch *M*, perhaps because of the *M-S* error shown in Fig. 1c.

4. Equilibration from one stable equilibrium to another

Using an OFF state equilibrium for one fixed value of *H* and then changing *H* from one value to another within the range of stable OFF states leads to transient behavior suitable for examination. Atlantic salinity $\overline{S}$ is expected to adjust to a new value appropriate to the new *H*. The evolution equation [Eq. (4), Part I] offers a prediction for this transient behavior. Here, the agreement between the evolution equation and the numerical model with respect to this transient behavior is examined.

Transient solutions to the evolution Eq. (4) $V_{\text{Atl}}(\partial\overline{S}/\partial t) = a\overline{S}^2 + b\overline{S} + c$ fall into two categories, depending on whether real roots exists. For real roots, $V_{\text{Atl}}(\partial\overline{S}/\partial t) = a(\overline{S} - \overline{S}_1)(\overline{S} - \overline{S}_2)$, where $\overline{S}_i$ are the roots of the polynomial $F_{\text{circ}}(\overline{S})$ [see Eq. (5), Part I], and again the naming of $\overline{S}_i$ is chosen so that $\overline{S}_1 \geq \overline{S}_2$, that is, $\overline{S}_1$ represents the unstable OFF branch, whereas $\overline{S}_2$ represents the stable OFF branch. it can be shown that for an initial salinity $\overline{S} = \overline{S}_0$, the solution to the evolution equation is

$$\overline{S}(t) = \frac{\overline{S}_1(\overline{S}_2 - \overline{S}_0)e^{-\alpha t} - \overline{S}_2(\overline{S}_1 - \overline{S}_0)}{(\overline{S}_2 - \overline{S}_0)e^{-\alpha t} - (\overline{S}_1 - \overline{S}_0)}, \qquad (1)$$

where $\alpha = a(\overline{S}_1 - \overline{S}_2) = 2\sqrt{a/V_{\text{Atl}}(F_s^* - F_s)}$. The system described by this function encounters a singularity at some $t = t^*$ when the denominator is 0. That is, $e^{-\alpha t} = \overline{S}_1 - \overline{S}_0/\overline{S}_2 - \overline{S}_0$ is approached as $t \to t^*$. For this equation to be valid, the second term needs to be positive (as the exponential term is always positive). In other words, either $\overline{S}_0 < \overline{S}_1$ and $\overline{S}_0 < \overline{S}_2$, or $\overline{S}_0 > \overline{S}_1$ and $\overline{S}_0 > \overline{S}_2$. Of these two possibilities, only the second ($\overline{S}_0 > \overline{S}_1$) leads to a positive t^*. This behavior is of course in agreement with our considerations in Part I. For all initial conditions $\overline{S}_0 < \overline{S}_1$ (i.e., smaller than the unstable equilibrium $\overline{S}$), let $e^{-\alpha t} = 0$ in Eq. (8) to find the asymptotic end state $\overline{S}_2$ of the system, so all $\overline{S}_0 < \overline{S}_1$ evolve toward the stable OFF branch. Other initial conditions evolve toward the ON state.

To examine how well the evolution to the stable OFF branch described by Eq. (1) agrees with the behavior of the model, a stable OFF state equilibrium can be taken in the model at $H = 0$ Sv and apply a constant $H = 0.0160$ Sv from thereon to examine the transient behavior as it equilibrates toward its new steady OFF state. The transient behavior should be described by Eq. (1), where initial and final conditions $\overline{S}_0$ and $\overline{S}_1$ known from the model are used. The climate amplification $\beta = 0.25$ (see Fig. 3, Part I) should be taken into account, where an initial increase δH in *H* eventually leads to an increase $\delta F_s = (1 + \beta)\delta H$ in the total net Atlantic salt flux. This affects the rate of evolution but not the final state. The climate amplification effect can be incorporated into the coefficient α of time *t*. We use an averaged term $\alpha = 2\sqrt{a\{F_s^* - [H(1 + \tfrac{1}{2}\beta)]\}}$, where $H = 0.0160$ Sv. It can be shown that this is expected to lead to an error in equilibration rate (and time) of less than 6%. Furthermore, $\overline{S}_0 = 34.28\,\text{kg}\,\text{m}^{-3}$ (the Atlantic salinity at $H = 0$), $\overline{S}_1 = 34.37\,\text{kg}\,\text{m}^{-3}$ (the salinity at $F_s = 0.0160$ Sv, see Part I) and $\overline{S}_2 = 3\overline{S}^* - 2\overline{S}_1$. Also, $a = \upsilon_1 d_1 = 0.4404$ $\text{m}^6\ \text{kg}^{-1}$. The transient behavior of Atlantic salinity $\overline{S}$ (Fig. 2a) is captured well by Eq. (1), with a small but noticeable error in the first 1000 years. In contrast (Fig. 2b), almost no perceptible error occurs when comparing the behavior of the AAIW reverse cell in the model and the calculated *M* [computed via Eq. (2)]. The *M-S* error

Unauthenticated | Downloaded 04/20/21 11:40 AM UTC

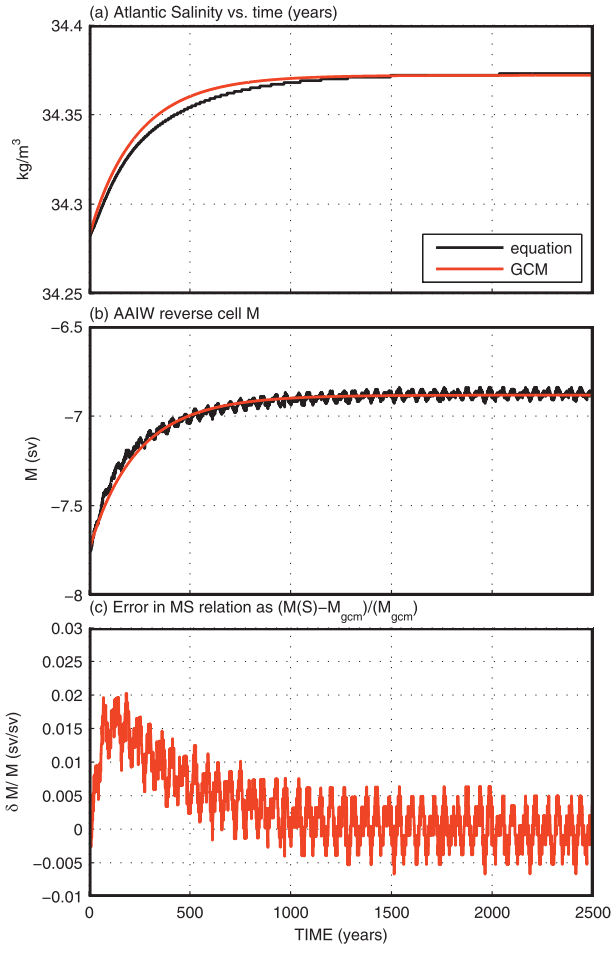

FIG. 2. Results of equilibrating the numerical model under a fixed anomalous flux H, starting from an equilibrium OFF state near the critical H^*. (a) Atlantic salinity $\overline{S}$ as a function of time t for the numerical model (red) and calculated using Eq. (1) (black). (b) The AAIW reverse cell strength M as a function of time t for the numerical model (red) and calculated using Eq. (1) (black). (c) The error indicator $[M(\overline{S}) - M_{\text{gcm}}]/M_{\text{gcm}}$, where $M(\overline{S})$ is M calculated from $\overline{S}$ via Eq. (2) (Part I), and M_{gcm} is the AAIW reverse cell strength diagnosed from the numerical model, as in the previous figure. Time values are in thousands of years.

indicator (see explanation of Fig. 1) shown in Fig. 2c takes a maximum value around 0.015 in the first few hundred years, but is generally negligible. This indicates that basic Eq. (2) of Part I holds well, and that the source of the deviation in the transient behavior of the Atlantic salinity is likely caused by a violation of Eq. (1) and/or Eq. (3) of Part I. The change in surface salt flux H occurs in the North Atlantic, and the discrepancy seen in Fig. 2a may be related to the time it takes for the associated salinity anomaly to travel to the South Atlantic and influence F_r and F_m. Nonetheless, the model clearly behaves in a very similar fashion to that described by Eq. (1), and predictions can be made using this equation.

5. Duration of transition from the OFF state to the ON state

The coefficient $2\sqrt{a/V_{\text{Atl}}(F_s^* - F_s)}$ appearing in Eq. (1) becomes small when F_s approaches F_s^* while $F_s < F_s^*$. This means the Atlantic salinity $\overline{S}$ evolves more slowly toward its equilibrium value near F_s^*. This is in agreement with our numerical model runs close to F_s^*, which needed to be run for several tens of thousands of years to equilibrate. This arises from a weak feedback between δF_{circ} and $\delta\overline{S}$ (see Part I) due to a small slope $\partial F_{\text{circ}}/\partial S$, where F_{circ} evolves very slowly to match F_s (after increasing F_s from a lower F_s^0). This feedback should also be weak for F_s close to F_s^* and $F_s > F_s^*$, leading to a slow collapse of the OFF state, and the emergence of the ON state.

To examine the emergence of the ON state for $F_s > F_s^*$, a set of experiments have been conducted where an OFF state equilibrium close to F_s^* (associated with H^*) is equilibrated with respect to a new unstable $H > H^*$. Figure 3 shows the time development of several key parameters in one of these numerical experiments where H is close to H^*. The AAIW reverse cell strength M in the model (Fig. 3a) shows a very slow initial decline in M accompanied by a slow increase in Atlantic salinity (Fig. 3c), followed by a rapid collapse of the AAIW reverse cell toward the end. The rapid collapse is accompanied by the sudden emergence of the NADW cell (Fig. 3b). The NADW value shown is measured as the maximum in the meridional streamfunction in the North Atlantic below the wind-driven surface layers. The error indicator (shown in Fig. 3d, see above for explanation) remains remarkably small throughout the process, where the error is negligible up to year 45 000. After that, a kink occurs in $\overline{S}$ and M leading into a regime of noticeably faster decline in M (Figs. 3a,c). However, the error indicator remains small throughout the rest of the integration period, indicating that the kink around year 45 000 does not yet herald a violation of the relationship between M and S of Eq. (2) (Part I). Subsequently at approximately year 50 000, the error indicator inflates rapidly when strong NADW formation appears near the end of the integration period. The relationship between M and $\overline{S}$ in Eq. (2) (Part I) becomes significantly violated only when strong NADW formation appears at the very end of the integration period, indicating the emergence of a new regime.

We can calculate the time it takes for an OFF state to give way to an ON state when F_s is increased above F_s^* from a certain value for a stable F_s just below F_s^*. It can be shown that for $F_s > F_s^*$ (where no real roots $\overline{S}_i$ exist for $F_{\text{circ}} = 0$), the Atlantic salinity evolves as

Unauthenticated | Downloaded 04/20/21 11:40 AM UTC

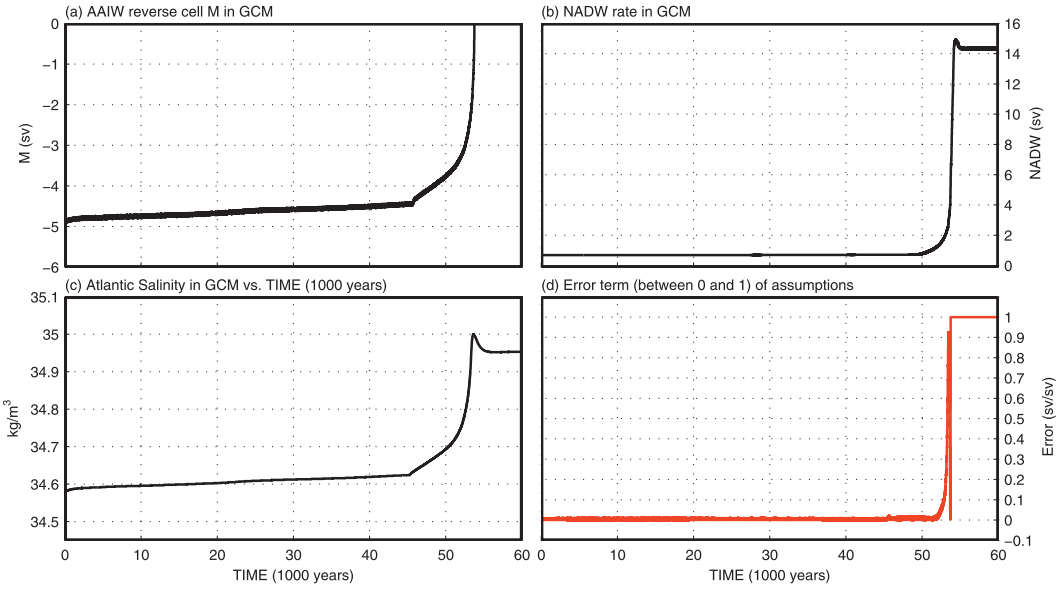

FIG. 3. Time-dependent numerical model behavior of the OFF state in response to a small increase in anomalous North Atlantic salt flux H from just below the critical value H^* to just above H^*. The initial (stable) $H = 0.0359$ Sv. (a) The AAIW reverse cell strength M. (b) The NADW cell strength. (c) The average Atlantic salinity $\overline{S}$. (d) The error indicator (as calculated in previous figures).

$$\overline{S}(t) = \overline{S}^* + K\tan\{V_{\mathrm{Atl}}^{-1}aKt + a\tan[K^{-1}(\overline{S}_0 - \overline{S}^*)]\}, \tag{2}$$

where $K = \sqrt{(F_s - F_s^*)/a}$. The term $a\tan[K^{-1}(\overline{S}_0 - \overline{S}^*)]$ can be neglected when choosing the initial $\overline{S}_0$ close to the critical $\overline{S}^*$. The coefficient of time t is $V_{\mathrm{Atl}}^{-1}\sqrt{(F_s - F_s^*)a}$, again predicting slow integration times near F_s^*. Calculating the time t^* needed to reach the first singularity of the tan function, it can be shown that the reverse cell collapse times are given by

$$t^* = \frac{\pi}{2}\frac{V_{\mathrm{Atl}}}{aK} = \frac{\pi V_{\mathrm{Atl}}}{2\sqrt{a(F_s - F_s^*)}}. \tag{3}$$

Figure 4 shows these integration times as a function of the added anomalous salt flux ΔH relative to an stable equilibrium OFF state close to H^*. Also shown are the model OFF-state-collapse times as a function of ΔH, where the time to an OFF-state collapse is defined as the time it takes for the reverse cell strength to become 0. Here, the climatic feedback is ignored, which may introduce errors between 0.2 and 0.4.

The times needed for the reverse cell to disappear agree very well with Eq. (3) for $\Delta H > 1.5 \times 10^{-3}$ Sv, and deviate more significantly close to the singularity. The deviations in integration times may arise from additional dynamical effects overlooked by our approach. These unknown factors appear to smear the predicted t^* curve in the direction of H. Nonetheless, Eq. (3) captures the general behavior of the strongly increasing integration times around H^* and so provides insight into the reason behind these long evolution times.

Equation (3) suggests that H^* can be approached arbitrary closely, leading to arbitrary large decay times. However, an exceedingly small change δF_s in F_s is not

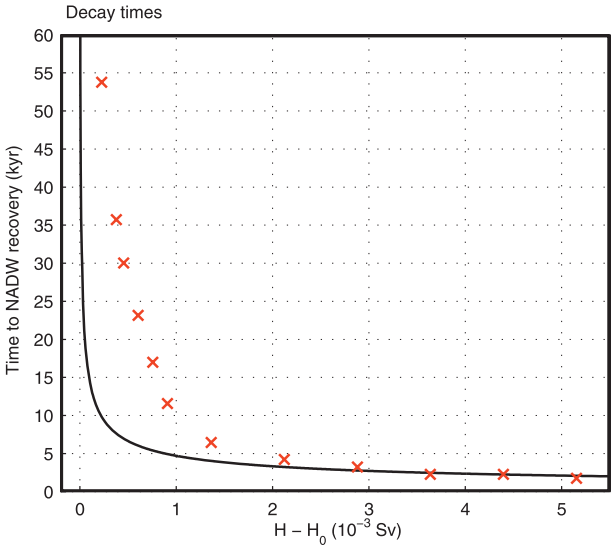

FIG. 4. Time elapsed before collapse of the OFF state in response to an increase ΔH in anomalous North Atlantic salt flux H from just below the critical value H^* to just above H^*. The initial (stable) $H_0 = 0.0359$ Sv. Shown against the difference in $H - H_0$ is the collapse time t^* shown in Eq. (3) (black). The collapse times found in the numerical model are marked with a red x symbol.

Unauthenticated | Downloaded 04/20/21 11:40 AM UTC

meaningful because of the background noise level in F_s in the model. Inevitable perturbations of the OFF state at H^* should render its decay time finite. We attempted to compute the collapse time t^*_{noise} in the presence of noise by replacing H with a normally distributed $H + \delta H$ around H in Eq. (3). A standard deviation in H similar to that of F_s corresponds to a 46 000 year maximal decay time. Decay times in excess of 54 000 years were found in the model. The main point here is that noise in the model should provide an upper bound to integration times. Note that here $\partial F_{\text{cric}}/\partial \overline{S} < 0$ becomes the condition for stable OFF states.

6. Summary and conclusions

In Part I the closed Atlantic salt budget $F_{\text{circ}}(\overline{S}) + F_s = 0$ and the ability to express the total oceanic salt flux F_{circ} as a function of the average upper Atlantic salinity $\overline{S}$ allowed the formulation of a simple evolution equation [Eq. (4) in Part I, see Table 2 here] for $\overline{S}_t$ for all fixed F_s. This equation describes the time-dependent behavior of $\overline{S}_t$. We have tested this evolution equation by examining the transient behavior of its solutions. We find that the predictions generally hold as long as the basic premises stated in Part I are valid. The premises hold for several interesting transient cases. The unstable equilibria S_{unst} that mark the upper boundary of the OFF state attraction basin are elucidated by the transient behavior shown here. Nonsingular solutions to the evolution equation offer an excellent description of the transient equilibration from one stable NADW OFF state to another in response to a change in the anomalous salt flux H. We have also incorporated the effect of the climate amplification described in Part I in this experiment. Finally, unstable solutions to the evolution equation offer a good description of the distribution of decay times for the NADW OFF state around the critical surface flux H^*. These long times to collapse for H close to H^* arise from the very small slope of F_{circ} with respect to $\overline{S}$ in this neighborhood. In general, small changes in salinity can be linked to changes in the oceanic salt flux via $\delta F_{\text{circ}} = (\partial F_{\text{circ}}/\partial \overline{S})\delta \overline{S}$. This equation can be solved because anomalies in the average salinity $\overline{S}$ evolve as $(\partial/\partial t)\delta \overline{S} = \delta F_{\text{circ}}$ around any $\overline{S}$ where the flux balance holds. That is, the initial behavior of small $\delta \overline{S}$ can be approximated by exponential growth–decay at a rate $\delta F_{\text{circ}}/\partial \overline{S}$ evaluated at $\overline{S}$. The small $\delta F_{\text{circ}}/\partial \overline{S}$ around $\overline{S}^*$ when H is close to H^* therefore implies very slow initial growth for small positive salinity anomalies $\delta \overline{S}$. The growth of positive anomalies $\delta \overline{S}^*$ leads to the collapse of the OFF state. Exceedingly long collapse times greater 50 000 years are found for surface flux values slightly in excess of the critical value. As a consequence, care needs to be taken around the critical flux H^* in hysteresis experiments where the anomalous flux is slowly varied to take the system through a bistable trajectory.

Note that our experiments have dealt with perturbations to the NADW OFF state alone. It is unclear whether the unstable equilibria $\overline{S}_{\text{unst}}$ would be a reliable indicator for collapse when approached from an ON state, where NADW dynamics modify model behavior. We therefore limit this paper to variations around the NADW OFF state and emphasize that our approach is generally not expected to be valid when ON state dynamics are at play. NADW ON state dynamics that complicate the application of our evolution equation there are North Atlantic temperature effects and the significant meridional redistribution of thermocline salt arising from the NADW circulation. Also, the proportionality between the reverse cell strength M and the density contrast between the AAIW and the NADW formation regions is better in our OFF state than the analogous case for the NADW formation rate in ON, where it appears that a more crude linear relationship holds (figure not shown).

Our aim has been an understanding of the dynamics responsible for the existence of the NADW OFF state in models where the AAIW reverse cell has a significant influence on the Atlantic salt budget. In this case, the OFF state meridional circulation has a significant influence on AMOC bistability and the transient behavior of the model. We found that we can accurately calculate the maximal Atlantic salinity and salt flux where OFF states exist. We could do this because of a set of simplifying properties of the OFF state that also allowed us to derive simple and testable analytical solutions to the evolution equation of the system in the OFF state. The numerical experiments shown here indicate that this predicted transient behavior also corresponds well with the numerical general circulation model.

Acknowledgments. We thank the University of Victoria staff for support in usage of the their coupled climate model. This research was supported by the Australian Research Council and the Australian Antarctic Science Program. We thank Marc d'Orgeville for an internal review and Bruce Henry from the School of Mathematics at the University of New South Wales for help in deriving the time-dependent solutions [Eqs. (1) and (2)] to the evolution equation shown in Part II.

REFERENCES

Colin de Verdière, A., 2010: The instability of the thermohaline circulation in a low-order model. *J. Phys. Oceanogr.,* **40,** 757–773.

Unauthenticated | Downloaded 04/20/21 11:40 AM UTC

Gent, P. R., and J. C. McWilliams, 1990: Isopycnal mixing in ocean general circulation models. *J. Phys. Oceanogr.,* **20,** 150–155.

Kalnay, E., and Coauthors, 1996: The NCEP/NCAR 40-Year Reanalysis Project. *Bull. Amer. Meteor. Soc.,* **77,** 437–471.

Lucarini, V., and P. H. Stone, 2005a: Thermohaline circulation stability: A box model study. Part I: Uncoupled models. *J. Climate,* **18,** 501–513.

——, and ——, 2005b: Thermohaline circulation stability: A box model study. Part II: Coupled atmosphere–ocean model. *J. Climate,* **18,** 514–529.

Pacanowski, R., 1995: MOM2 documentation user's guide and reference manual. GFDL Ocean Group Tech. Rep. 3. 3rd ed. NOAA, GFDL, Princeton, 232 pp.

Rahmstorf, S., 1996: On the freshwater forcing and transport of the Atlantic thermohaline circulation. *Climate Dyn.,* **12,** 799–811.

Rooth, C., 1982: Hydrology and ocean circulation. *Prog. Oceanogr.,* **11,** 131–149.

Sijp, W. P., and M. H. England, 2006: Sensitivity of the Atlantic thermohaline circulation and its stability to basin-scale variations in vertical mixing. *J. Climate,* **19,** 5467–5478.

——, and ——, 2008: The control of polar haloclines by along-isopycnal diffusion in climate models. *J. Climate,* **21,** 6260–6282.

——, ——, and J. M. Gregory, 2012: Precise calculations of the existence of multiple AMOC equilibria in coupled climate models. Part I: Equilibrium states. *J. Climate,* **25,** 282–298.

Stocker, T., and A. Schmittner, 1997: Influence of CO2 emission rates on the stability of the thermohaline circulation. *Nature,* **388,** 862–865.

Weaver, A. J., M. Eby, E. C. Wiebe, and Coauthors, 2001: The UVic Earth System Climate Model: Model description, climatology, and applications to past, present, and future climates. *Atmos.–Ocean,* **39,** 1067–1109.

Zickfeld, K., T. Slawig, and S. Rahmstorf, 2004: A low-order model for the response of the Atlantic thermohaline circulation to climate change. *Ocean Dyn.,* **54,** 8–26.

Unauthenticated | Downloaded 04/20/21 11:40 AM UTC